Wavefronts, caustics, and ronchigrams of a spherical wave reflected by a spherical mirror

Jorge Castro-Ramos,[1] Magdalena Marciano-Melchor,[2] Mariana Marcelino-Aranda,[3] Edwin Román-Hernández,[4] José Guadalupe Santiago-Santiago,[5] Gilberto Silva-Ortigoza,[5,*] Ramón Silva-Ortigoza,[2] Román Suárez-Xique,[5] and José Miguel Zárate-Paz[5]

[1]*Instituto Nacional de Astrofísica, Óptica y Electrónica, Apartado Postal 51 y 216, Tonantzintla, Puebla, C.P. 72000, Mexico*

[2]*CIDETEC-IPN. Departamento de Posgrado. Área de Mecatrónica. Unidad Profesional Adolfo López Mateos, México, D.F., C.P. 07700, Mexico*

[3]*UPIICSA-IPN. Sección de Estudios de Posgrado e Investigación, México, D.F., C.P. 08400, Mexico*

[4]*Universidad del Istmo, Departamento de Matemáticas Aplicadas, Cd. Universitaria, Tehuantepec, Oax. C.P. 70760, Mexico*

[5]*Facultad de Ciencias Físico Matemáticas de la Benemérita Universidad Autónoma de Puebla, Apartado Postal 1152, Puebla, Pue. 72001, Mexico*

**Corresponding author: gsilva@fcfm.buap.mx*

Received October 17, 2012; accepted November 17, 2012;
posted December 12, 2012 (Doc. ID 177946); published January 10, 2013

The aim of the present work is twofold: first we obtain analytical expressions for both the wavefronts and the caustic associated with the light rays reflected by a spherical mirror after being emitted by a point light source located at an arbitrary position in free space, and second, we describe, in detail, the structure of the ronchigrams when the grating or Ronchi ruling is placed at different relative positions to the caustic region and the point light source is located on and off the optical axis. We find that, in general, the caustic has two branches: one is a segment of a line, and the other is a two-dimensional surface. The wavefronts, at the caustic region, have self intersections and singularities. The ronchigrams exhibit *closed-loop fringes* when the grating is placed at the caustic region.

OCIS codes: 080.0080, 120.5700, 110.4190, 220.4840.

1. INTRODUCTION

The spherical mirror is one of the most used components to construct optical devices and to carry out a variety of experiments. For these reasons, a natural and fundamental question is, "How do we determine the quality of a real polished mirror?" To answer this question, not only for a spherical mirror but also for an arbitrary optical system, there has been a development of several tests [1,2]. The Ronchi test [3,4], developed by Ronchi in the 1920s, is one of those. The basic idea of this test is to deduce the quality of an optical system by comparing a *real* pattern, referred to as the real ronchigram, obtained from the experiment, with the *ideal* one, obtained by simulation assuming that all the characteristics of the ideal optical system that we want to construct are known. Therefore, as remarked by Ronchi himself, a clear understanding of the properties of the ideal ronchigram is crucial to apply this test. Thus, there has been considerable research on the simulation of ronchigrams for spherical and aspherical mirrors [5–11] (see also [4] and the references cited therein). It is important to point out that the Ronchi test is established in a quantitative way only when the grating or Ronchi ruling is placed off the caustic region. This is so because in that case the ronchigram does not contain any closed-loop fringes and thus it is easy to carry out the comparison between the real and ideal fringes. However, the most important feature associated with the reflected light rays by the spherical mirror after being emitted by a point light source placed at a determined position in space is its set of *focal points* or caustic surface, so we claim that working at the caustic region the sensitivity of the Ronchi test will be improved and thus a clear description of the ronchigram when the grating is placed at the caustic region is needed. In a recent work [12], by using the caustic touching theorem established by Berry [13] and the geometrical point of view of the Ronchi test, we discovered that the caustic associated with the reflected light rays play a major role in the computation of the ideal ronchigram. We remarked that the closed-loop fringes observed in the ronchigram can be interpreted as a disruption of shadows and that they appear when the grating touches the caustic region. The general results were applied to a spherical mirror when the point light source is located on the optical axis. In this work we use our general equations obtained in [12,14,15] to study the structure of the reflected wavefronts, caustics, and ronchigrams for a spherical mirror when the point light source is located at an arbitrary position of space. More explicitly, we obtain analytical expressions for the reflected wavefronts and the caustic when the point light source is located on and off the optical axis. With the knowledge of the caustic, we present a detailed study of the structure of the ronchigram when the grating is placed at the caustic region. These results complete the study started in [12] for a spherical mirror. The organization of this work is as follows: in Section 2, following [12,14], we present the basic equations to compute the reflected wavefronts, the caustic, and the

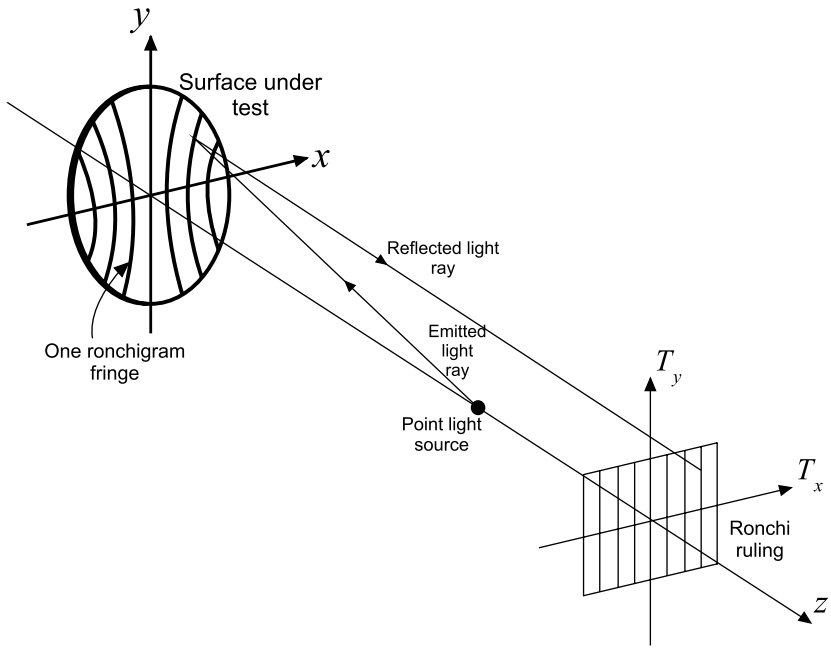

Fig. 1. Schematic drawing of the Ronchi test arrangement. In this diagram we have the surface under test, locally given by $z = f(x, y)$, a point light source located on the optical axis, and a Ronchi ruling. The pattern observed through the grating on the surface of the mirror is referred to as the real ronchigram.

ronchigram for an arbitrary configuration of the point light source, grating, and mirror. In Section 3 these general equations are applied to the spherical mirror and we obtain analytical compact expressions for the reflected wavefronts, the caustic, and the ronchigram. These analytical expressions are used to present a detailed description of the ronchigrams when the point light source is placed on and off the optical axis and the grating is placed at different relative positions to the caustic region. Finally, the conclusions are presented.

In this work, we consider the geometrical point of view of the Ronchi test. The essential features of this test for a concave mirror when the point light source is located on the optical axis may be described by reference to Fig. 1 [4,16]. The light rays emitted by the point light source are reflected by the mirror under test and they focus on a region in the space. This region is the caustic associated with the reflected light rays. The grating, also referred to as a Ronchi ruling, is located at different positions on the optical axis. The pattern observed through the grating on the surface of the mirror is referred to as the real ronchigram. From the geometrical point of view, the fringes of the real ronchigram are interpreted as shadows of the ruling bands. The defects of the mirror under test can be deduced by comparing the real fringes with the ideal ones, which are obtained by simulation assuming that the form of the ideal mirror and the position of both the point light source and grating are known [17].

2. BASIC RESULTS

In this section, following [12,14], we present the equations to compute the wavefronts and the caustic associated with the reflected light rays by an arbitrary smooth surface after being emitted by a point light source located at an arbitrary position in free space. Furthermore, we present the equations to simulate the ideal ronchigram for an arbitrary smooth reflector when the point light source and the grating are located at arbitrary positions.

A. Equations Describing the Reflected Wavefronts

Using a complete integral of the eikonal equation a direct computation shows that the wavefronts associated with the light rays reflected by an arbitrary smooth surface after being emitted by a point light source located at an arbitrary position $\mathbf{s} = (s_1, s_2, s_3)$ in free space are described by

$$\mathbf{X}(\mathbf{s}, x, y) = \mathbf{r}(x, y) + [C - |\mathbf{r}(x, y) - \mathbf{s}|]\hat{\mathbf{R}}(\mathbf{s}, x, y), \quad (1)$$

where $\mathbf{r} = (x, y, f(x, y))$ denotes the position of the point on the smooth curved reflector at which is reflected the light ray that is emitted by the point light source in the direction $\hat{\mathbf{I}}$, C denotes each one of the reflected wavefronts, and $\hat{\mathbf{R}}$ denotes the direction of the reflected light ray, which is computed using the reflection law and is explicitly given by

$$\hat{\mathbf{R}} = \frac{\mathbf{h}}{\alpha} \quad (2)$$

with $\mathbf{h} = (h_1, h_2, h_3)$ and

$$h_1 = (x - s_1)(1 - f_x^2 + f_y^2) - 2f_x[f_y(y - s_2) + s_3 - f], \quad (3)$$

$$h_2 = (y - s_2)(1 + f_x^2 - f_y^2) - 2f_y[f_x(x - s_1) + s_3 - f], \quad (4)$$

$$h_3 = (f - s_3)(-1 + f_x^2 + f_y^2) + 2[f_x(x - s_1) + f_y(y - s_2)], \quad (5)$$

$$\alpha = (1 + f_x^2 + f_y^2)\sqrt{(s_1 - x)^2 + (s_2 - y)^2 + (s_3 - f)^2}. \quad (6)$$

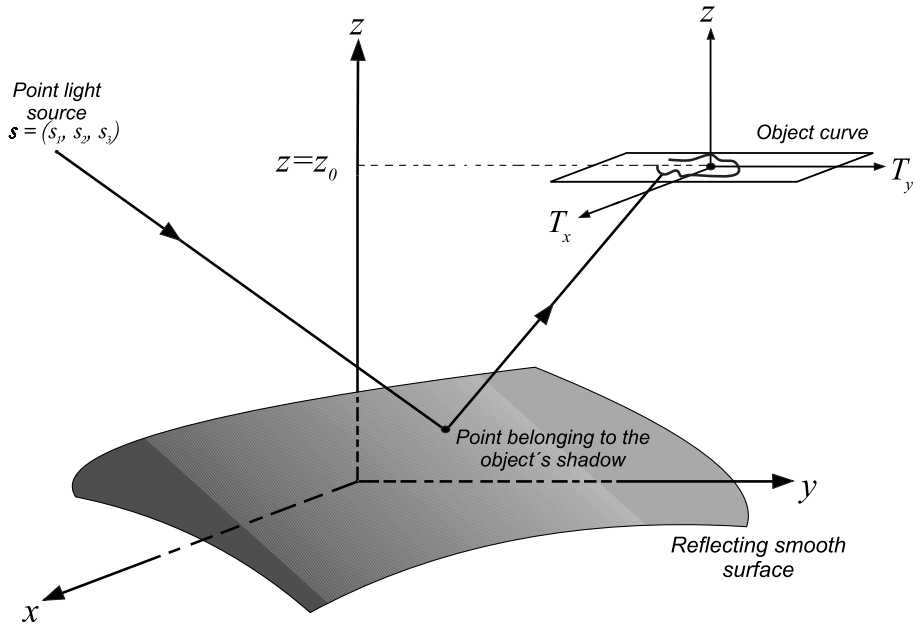

Fig. 2. Schematic drawing of the two sets of coordinate systems used to compute the image of a one-dimensional object obtained by reflection on an arbitrary smooth surface locally given by $z = f(x, y)$. We also have included an emitted light ray such that its associated reflected light ray connects a point of the smooth surface with a point of the one-dimensional object. The point, on the smooth surface, where the emitted light ray is reflected belongs to the shadow of the one-dimensional object.

B. Caustic Associated with the Reflected Wavefronts

If the position of the point light source is assumed to be known; that is, if **s** is given, then from a mathematical point of view Eq. (1) describes a map between two subsets of R^3, where (x, y, C) are the coordinates labeling the points in the domain space and (X, Y, Z) are local coordinates in the target space. In general, there is a region in the space where the reflected wavefronts will be singular or equivalently the reflected light rays will focus. This region is referred to as the caustic associated with the reflected wavefronts or reflected light rays. By definition, the caustic [18–20] is the image of the critical set of the map (1). The critical set is the set of points in the domain space where the map is not locally one to one. In our case, it is given by

$$C = C_{\pm}(x, y) \equiv |\mathbf{r} - \mathbf{s}| + \alpha\left(\frac{-H_1 \pm \sqrt{H_1^2 - 4H_2H_0}}{2H_2}\right), \tag{7}$$

where

$$H_0 = \mathbf{h} \cdot \left[\left(\frac{\partial \mathbf{r}}{\partial x}\right) \times \left(\frac{\partial \mathbf{r}}{\partial y}\right)\right],$$
$$H_1 = \mathbf{h} \cdot \left[\left(\frac{\partial \mathbf{r}}{\partial x}\right) \times \left(\frac{\partial \mathbf{h}}{\partial y}\right) + \left(\frac{\partial \mathbf{h}}{\partial x}\right) \times \left(\frac{\partial \mathbf{r}}{\partial y}\right)\right],$$
$$H_2 = \mathbf{h} \cdot \left[\left(\frac{\partial \mathbf{h}}{\partial x}\right) \times \left(\frac{\partial \mathbf{h}}{\partial y}\right)\right], \tag{8}$$

and the caustic, which is obtained substituting Eq. (7) into Eq. (1), is given by

$$\mathbf{X} = \mathbf{X}_{c\pm} = \mathbf{r} + \left(\frac{-H_1 \pm \sqrt{H_1^2 - 4H_2H_0}}{2H_2}\right)\mathbf{h}. \tag{9}$$

From this equation, it is clear that when $H_2 \neq 0$, the caustic associated with the reflected wavefronts described by Eq. (1), in general, is composed by two branches, which for very particular forms of the reflecting surface and particular positions of the point light source reduce to a single point. For example,

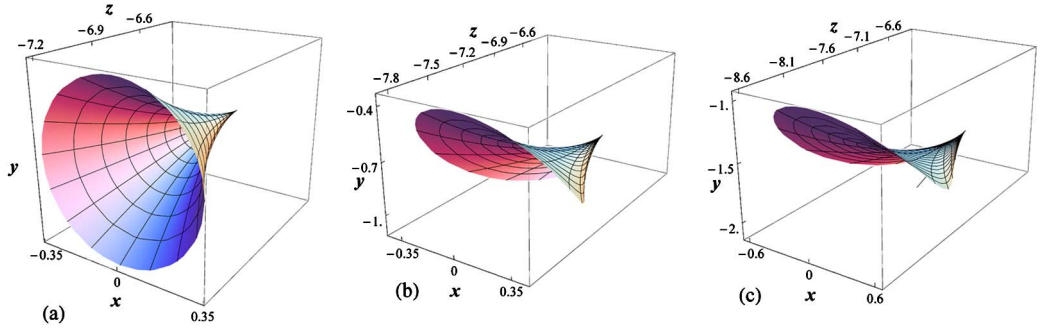

Fig. 3. (Color online) Caustic given by Eqs. (28) and (29) when the point light source is placed at (a) (0, 0, and 13.5 cm), (b) (2, 0, and 13.5 cm), and (c) (4, 0, and 13.5 cm).

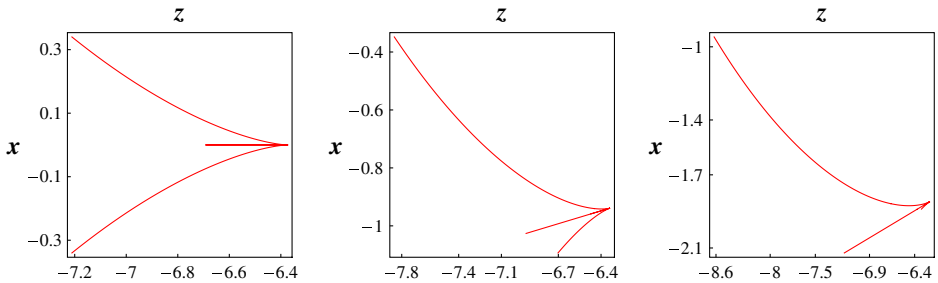

Fig. 4. (Color online) Intersections of the caustic surface, given by Eqs. (28) and (29), with the plane $y = 0$ when the point light source is placed at (a) (0, 0, and 13.5 cm), (b) (2, 0, and 13.5 cm), and (c) (4, 0, and 13.5 cm).

this happens when the reflecting surface is part of a spherical mirror and the point light source is located at the center of the mirror (see Section 3). In the general case, the two branches of the caustic are two-dimensional surfaces, and when they are stable under small deformations of the reflecting surface and the position of the point light source, they locally have singularities of well-known types: the swallowtail, the pyramid or elliptic umbilic, and the purse or hyperbolic umbilic [18–20]. From the results presented in Section 3, we conclude that the caustic associated with the reflected wavefronts, for a spherical mirror when the point light source is located either on or off the optical axis, is not stable under a local deformation of the spherical surface.

C. Equations to Compute the Ideal Ronchigram

Equation (1) describes the reflected wavefronts and also the reflected light rays. Observe that for fixed values of x and y this equation provides the parametric representation of a reflected light ray. In this parametrization each point on the reflected light ray is labeled by a particular value of C. Since we are interested in computing the ronchigram of a Ronchi ruling placed at a particular plane $Z =$ constant, it is convenient to use other more appropriate parametrization for the reflected light rays. To this end, we take $Z = z_0$, where z_0 is another coordinate. Therefore, Eq. (1) can be rewritten in the following form:

$$\begin{aligned} X(x,y,z_0) &= x + [z_0 - f(x,y)]\left(\frac{h_1(x,y,\mathbf{s})}{h_3(x,y,\mathbf{s})}\right), \\ Y(x,y,z_0) &= y + [z_0 - f(x,y)]\left(\frac{h_2(x,y,\mathbf{s})}{h_3(x,y,\mathbf{s})}\right), \\ Z(x,y,z_0) &= z_0, \end{aligned} \tag{10}$$

where now z_0 labels the points on the reflected light rays and is such that for fixed values of x and y, $f(x,y) \le z_0 < \infty$. A direct computation shows that the caustic associated with this map is also given by Eq. (9). This is so, because Eqs. (1) and (10) are two different representations of the same reflected light rays and the caustic is an *observable entity*; that is, it is independent of the coordinated system used to compute it. Equation (1) provides directly the wavefronts associated with the reflected light rays, while Eq. (10) are more appropriate to compute the ronchigram, as we will see later on.

Observe that for a fixed position of the point light source Eq. (10) describe the parametric representation of a map between two subsets of R^3, where (x,y,z_0) are the coordinates labeling the points in the domain space and (X,Y,Z) are local coordinates in the target space. Equivalently, Eq. (10), can be seen as a *one-parameter* family of maps between subsets of R^2, where each map is characterized by a particular value of z_0. This family is explicitly given by

$$\begin{aligned} X(x,y) &= x + [z_0 - f(x,y)]\left(\frac{h_1(x,y,\mathbf{s})}{h_3(x,y,\mathbf{s})}\right), Y(x,y) \\ &= y + [z_0 - f(x,y)]\left(\frac{h_2(x,y,\mathbf{s})}{h_3(x,y,\mathbf{s})}\right). \end{aligned} \tag{11}$$

Each member of the family, characterized by a specific value of z_0, maps points of the reflecting surface to points on the plane $Z = z_0$. It is important to remark that in Eq. (11), z_0 is not a coordinate as it is in Eq. (10), but it is a parameter characterizing a particular member of the family of maps, and is such that for fixed values of x and y, $f(x,y) \le z_0 < \infty$.

To compute the image of a one-dimensional object lying on the $Z = z_0 =$ constant plane, we introduce in that plane a second coordinate system (T_x, T_y), with origin at $(0,0,z_0)$ such that T_x and T_y are parallel to the axes X and Y, respectively (see Fig. 2). A one-dimensional object lying on this plane can be described in a parametric way by

$$\begin{aligned} T_x &= \Gamma(\sigma), \\ T_y &= \Sigma(\sigma), \end{aligned} \tag{12}$$

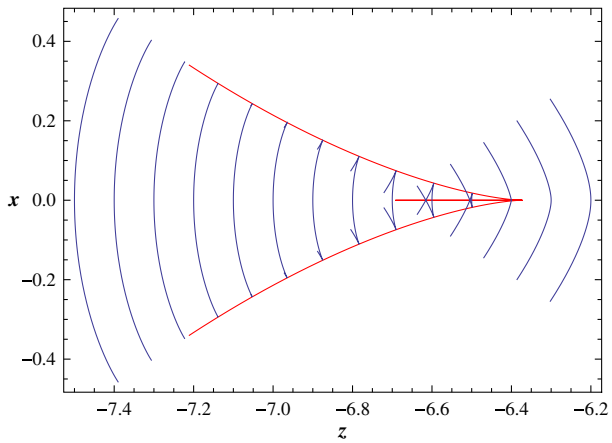

Fig. 5. (Color online) Intersections of some reflected wavefronts and the caustic surface, with the plane $y = 0$ when the point light source is placed at (0, 0, and 13.5 cm).

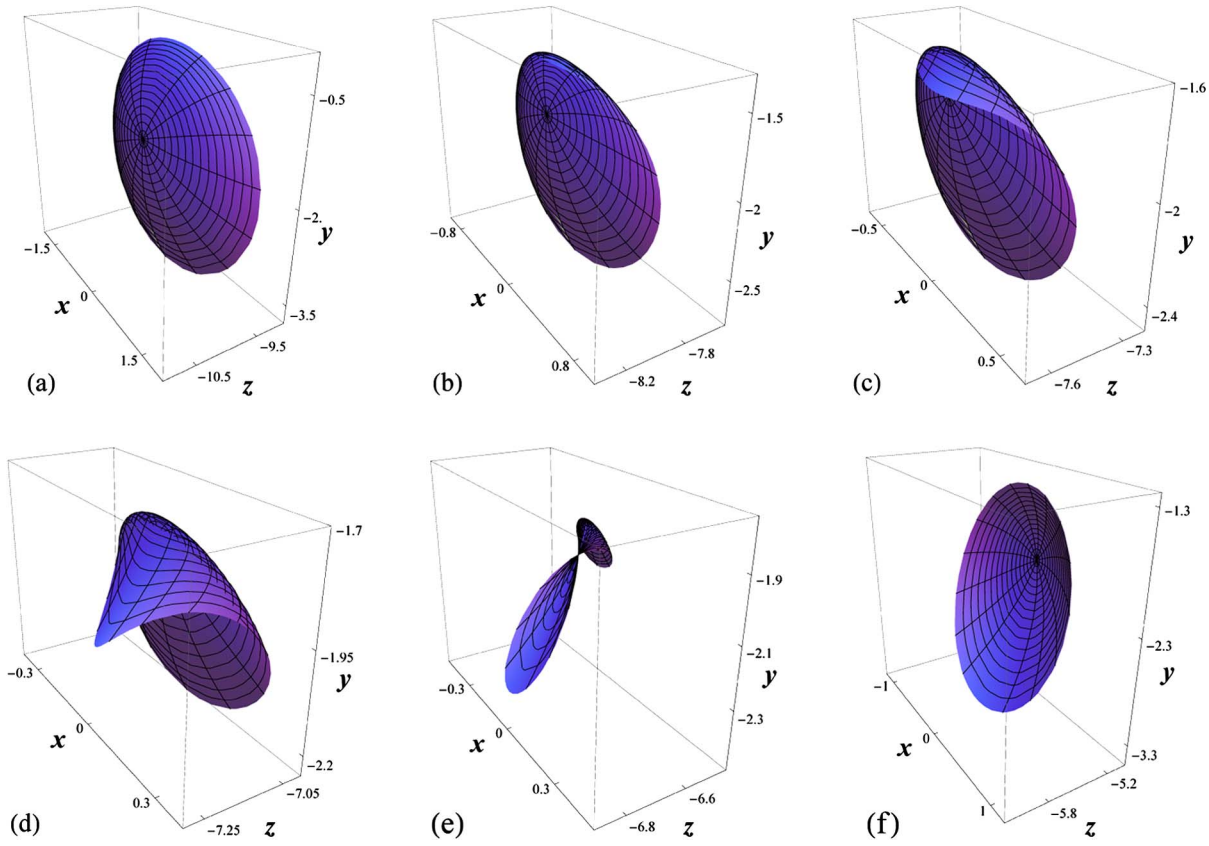

Fig. 6. (Color online) Some reflected wavefronts when the point light source is placed at (4, 0, and 13.5 cm). Observe that the wavefronts are smooth surfaces out of the caustic region [(a) and (f)], while at the caustic region they are singular [(b)–(e)].

where σ is a parameter that labels the points on the object. If we eliminate the parameter σ, we have that the object could be described by

$$T_y = \Lambda(T_x). \tag{13}$$

Therefore, all the points on the reflecting surface that are connected by a reflected light ray with the points of the one-dimensional object given by Eq. (12), located on the plane $Z = z_0$, are given by $(x, y, f(x, y))$, where x and y are solutions to

$$T_x(\sigma) = x + [z_0 - f(x,y)]\left(\frac{h_1(x,y,\mathbf{s})}{h_3(x,y,\mathbf{s})}\right),$$
$$T_y(\sigma) = y + [z_0 - f(x,y)]\left(\frac{h_2(x,y,\mathbf{s})}{h_3(x,y,\mathbf{s})}\right) \tag{14}$$

with the restrictions $x_{\min} \le x \le x_{\max}$ and $y_{\min} \le y \le y_{\max}$. (Since we are assuming that the curved reflector, the position of the point light source, and the object are known, then in these equations the unknown variables are x and y.)

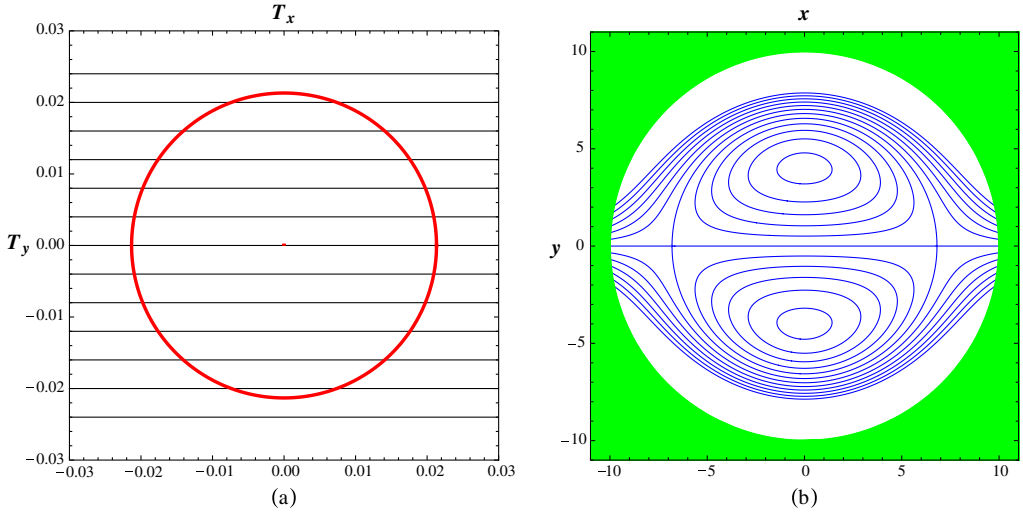

Fig. 7. (Color online) (a) Object space: the grating or Ronchi ruling and the caustic, which is a circle of radius $R_a = 0.0213$ cm and its center. (b) Image space: the associated Ronchigram. In this case $\mathbf{s} = (0, 0,$ and 13.5 cm) and the grating is placed at the plane $z = -6.51$ cm.

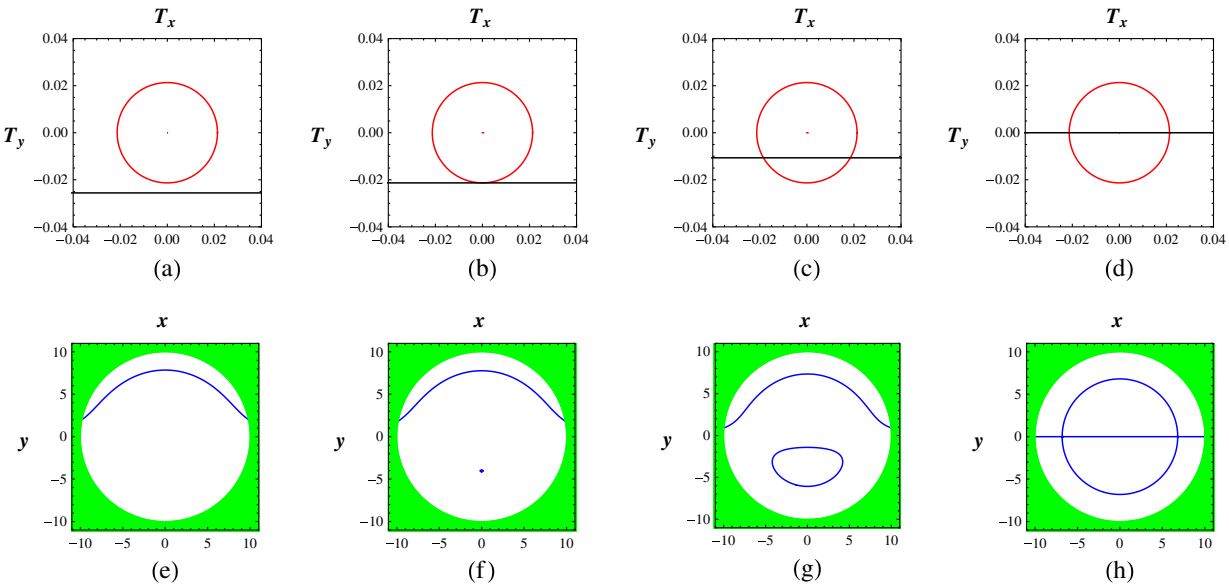

Fig. 8. (Color online) (a)–(d) Object space and (e)–(h) image space for $nd = -(1.2)R_a, -R_a, -R_a/2$, and 0, respectively. In this case $\mathbf{s} = (0, 0,$ and 13.5 cm) and the grating is placed at the plane $z = -6.51$ cm.

Therefore, if in free space we have a point light source located at $\mathbf{s}$ and a smooth mirror described by $\mathbf{r} = (x, y, f(x, y))$; then the *shadow* on the reflecting mirror of the one-dimensional object given by Eq. (12) is described by $(x, y, f(x, y))$, where x and y are solutions to Eq. (14) (see Fig. 2). In accordance with the caustic touching theorem, the relative position between the object and the caustic is crucial to compute the shadow of the object. Remember that the map given by Eq. (11) maps points on the reflecting surface to points on the plane $Z = z_0$. If the plane $Z = z_0$, which contains the object, is outside the caustic region—that is, there is no intersection between this plane and the caustic given by Eq. (9)—then the map (11) is locally one to one. This means that for each point $(T_x(\sigma), T_y(\sigma), z_0)$ on the object there is a unique solution (x, y) to Eq. (14) and therefore, under this condition, the shadow on the reflecting surface of the object is a curve. Now we assume that the plane $Z = z_0$ is located at the caustic region given by Eq. (9). In this second case, the map given by Eq. (11) is not locally one to one at those points that belong to the intersection of the caustic and the plane $Z = z_0$. Therefore, if the object lying on this plane is outside the caustic region, then we have the previous case, but if the object reaches the caustic in such a way that they become tangent to each other—that is, there is a touch between them—then in accordance with the caustic touching theorem, there will be shadow disruption. Such disruption may be elliptic, loop born from an isolated point, or hyperbolic, loop pinched off from an already existing one. In these cases, the object and its shadow do not have the same topology, and then we may see several shadows corresponding to a single object.

In this work we are interested in the case when the one-dimensional object is one of the rulings belonging to a Ronchi ruling. In other words, we are interested in computing the ruling shadows. To this end, we assume that in the plane $Z = z_0$ we place a Ronchi ruling with its rulings making an angle, Θ, with the positive T_x axis such that the distance between two adjacent rulings is d. That is, we assume that the Ronchi ruling is described by

$$T_y = T_x \tan\Theta + nd, \tag{15}$$

where $n = \pm 1, \pm 2 \ldots,$.

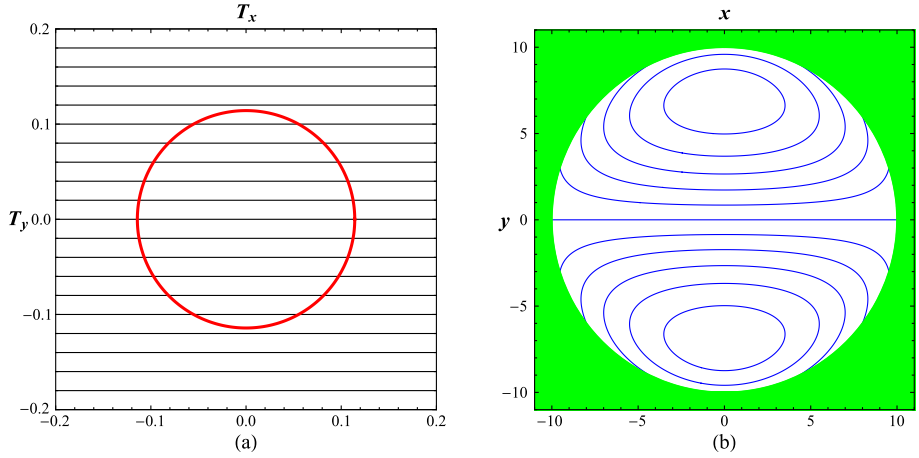

Fig. 9. (Color online) (a) Object space: the grating or Ronchi ruling and the caustic, which is a circle of radius $R_b = 0.1142$ cm. (b) Image space: the associated Ronchigram. In this case $\mathbf{s} = (0, 0,$ and 13.5 cm) and the grating is placed at the plane $z = -6.79$ cm.

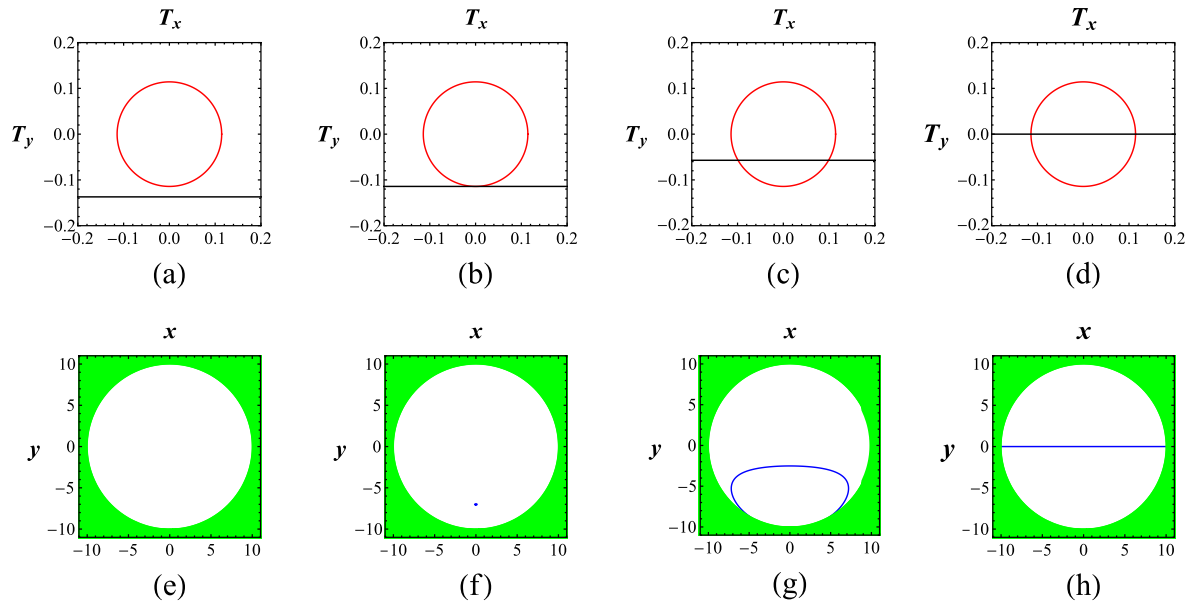

Fig. 10. (Color online) (a)–(d) Object space and (e)–(h) image space for $nd = -(1.2)R_b, -R_b, -R_b/2$, and 0, respectively. In this case $\mathbf{s} = (0, 0,$ and 13.5 cm) and the grating is placed at the plane $z = -6.79$ cm.

From Eqs. (14) and (15), we find that for each value of n the fringes or shadows on the ronchigram are computed by solving for x and y the following equation:

$$y + [z_0 - f(x,y)]\left(\frac{h_2(x,y,\mathbf{s})}{h_3(x,y,\mathbf{s})}\right) = \left\{x + [z_0 - f(x,y)]\left(\frac{h_1(x,y,\mathbf{s})}{h_3(x,y,\mathbf{s})}\right)\right\}\tan\Theta + nd. \quad (16)$$

In the next section we solve this equation for a spherical mirror when the point light source is located on and off the optical axis.

It is important to remark that due to practical purposes it is more convenient to plot the simulated ronchigrams in a plane. Therefore, in this work we plot the ronchigrams in the plane $Z = 0$.

3. SPHERICAL MIRROR

In this section we obtain analytical expressions for the reflected wavefronts and the caustic for a spherical mirror when the point light source is located on and off the optical axis. Furthermore, using the caustic, we study the structure of the ronchigram when the grating or Ronchi ruling is located at different relative positions to the caustic associated with the reflected light rays. To this aim, we assume that

$$f = -\sqrt{a^2 - x^2 - y^2},$$
$$\mathbf{r} = \left(x, y, -\sqrt{a^2 - x^2 - y^2}\right), \quad (17)$$

where a is the radius of the sphere.

A. Equations Describing the Reflected Wavefronts

Using Eqs. (3)–(5) and (17) a direct computation shows that for this case

$$\mathbf{h} = \left(\frac{1}{f^2}\right)[2(\mathbf{s}\cdot\mathbf{r})\mathbf{r} - a^2(\mathbf{s}+\mathbf{r})], \quad (18)$$

$$\alpha = \frac{|\mathbf{s}-\mathbf{r}|a^2}{f^2}, \quad (19)$$

$$\hat{\mathbf{R}} = \frac{[2(\mathbf{s}\cdot\mathbf{r})\mathbf{r} - a^2(\mathbf{s}+\mathbf{r})]}{|\mathbf{s}-\mathbf{r}|a^2}. \quad (20)$$

Therefore, from Eqs. (1), (17), and (20), we find that the map that describes the reflected wavefronts for a spherical mirror when the point light source is located at an arbitrary position in free space is given by

$$\mathbf{X}(\mathbf{s},x,y) = \mathbf{r} + \frac{[C - |\mathbf{r}-\mathbf{s}|][2(\mathbf{s}\cdot\mathbf{r})\mathbf{r} - a^2(\mathbf{s}+\mathbf{r})]}{|\mathbf{r}-\mathbf{s}|a^2}. \quad (21)$$

A very particular case is when the point light source is located at the center of the mirror—that is, when $\mathbf{s} = (0,0,0)$. For this case Eq. (21) reduces to

$$\mathbf{X}(\mathbf{0},x,y) = (2a - C)\hat{\mathbf{r}}. \quad (22)$$

Therefore, the train of reflected wavefronts is a set of spheres. Each sphere is labeled by a particular value of C and has radius $|2a - C|$. Observe that $C \geq a$.

B. Caustic Associated with the Reflected Wavefronts

To compute the caustic associated with the map given by Eq. (21), we first use Eqs. (17) and (18) in Eq. (8) to obtain

$$H_0 = \left(\frac{a^2}{f^3}\right)[(\mathbf{s}-\mathbf{r})\cdot\mathbf{r}], \quad (23)$$

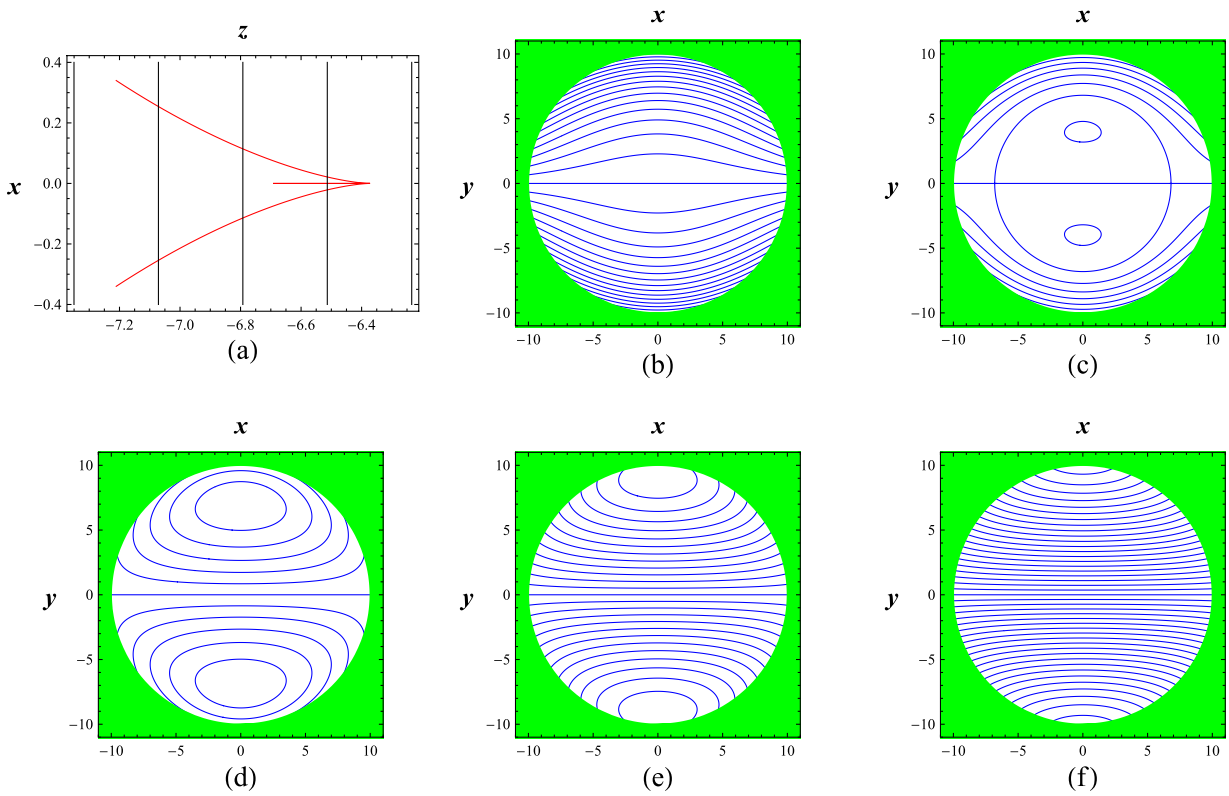

Fig. 11. (Color online) (a) Intersections of the caustic surface, given by Eqs. (28) and (29), when the point light source is placed at $\mathbf{s} = (0, 0,$ and 13.5 cm) and the planes $z =$ constant (where the Ronchi ruling is placed) with the plane $y = 0$. In (b)–(f) we present the ronchigrams when the grating is placed at the planes (b) $z = -6.23$ cm, (c) $z = -6.51$ cm, (d) $z = -6.79$ cm, (e) $z = -7.07$ cm, and (f) $z = -7.35$ cm, respectively.

$$H_1 = \left(\frac{2a^2}{f^5}\right)(\mathbf{s}-\mathbf{r})\cdot[a^2(\mathbf{s}-\mathbf{r}) + (\mathbf{s}\cdot\mathbf{r})\mathbf{r}], \tag{24}$$

$$H_2 = \left(\frac{a^4}{f^7}\right)\{|\mathbf{s}-\mathbf{r}|^2[3(\mathbf{s}\cdot\mathbf{r}) - a^2] + s^2[\mathbf{s}\cdot\mathbf{r} - a^2]\}, \tag{25}$$

where $s = \sqrt{(\mathbf{s}\cdot\mathbf{s})}$. Using Eqs. (17) and (23)–(25) in Eq. (7), a direct computation shows that the critical set is given by

$$C_- = \frac{2|\mathbf{r}-\mathbf{s}|[(\mathbf{s}-\mathbf{r})\cdot\mathbf{r}]}{(2\mathbf{s}-\mathbf{r})\cdot\mathbf{r}}, \tag{26}$$

$$C_+ = \frac{2|\mathbf{r}-\mathbf{s}|^3}{2s^2 - 3(\mathbf{s}\cdot\mathbf{r}) + a^2}. \tag{27}$$

In a similar manner using Eqs. (17) and (18) and Eqs. (23)–(25) in Eq. (9), we obtain that the caustic set can be written in the following form:

$$\mathbf{X}_{c-} = \frac{a^2\mathbf{s}}{(2\mathbf{s}-\mathbf{r})\cdot\mathbf{r}}, \tag{28}$$

$$\mathbf{X}_{c+} = \frac{2[a^2s^2 - (\mathbf{s}\cdot\mathbf{r})^2]\mathbf{r} + a^2[\mathbf{s}\cdot\mathbf{r} - a^2]\mathbf{s}}{a^2[a^2 + 2s^2 - 3(\mathbf{s}\cdot\mathbf{r})]}. \tag{29}$$

From Eqs. (28) and (29) we have that when the point light source is located at the center of the spherical mirror—that is, when $\mathbf{s} = (0, 0, 0)$—the caustic reduces to the point $(0, 0, 0)$, which is a well-known result. On the other hand, a direct computation shows that when $s_1 = 0$, $s_2 = 0$, $s_3 \to \infty$, $(x/a) \ll 1$, and $(y/a) \ll 1$—that is, in the paraxial approximation—the caustic reduces to $\mathbf{T}_{c\pm}(x, y) = (0, 0, -a/2)$, which is also a well-known result. This result implies that in the paraxial approximation of geometrical optics a plane wave incoming from infinity after reflection on a spherical mirror of radius a will focus to the point $(0, 0, -a/2)$; that is, the focal point in this case coincides with the caustic. From Eq. (28) we have the important result that, in general, this branch of the caustic is a segment of line and the other given by Eq. (29) is a two-dimensional surface.

It is important to point out that Burkhard and Shealy [21,22], and Theocaris [23,24] have presented a thorough study of the properties of the caustics obtained by illuminating any conic reflector with a point light source lying along the principal axis of the reflector (see also [25–27]). The main result obtained by these researchers was to present a description of the behavior of the properties of the caustic surface depending on the shape of the particular reflector, its aperture, and the relative position of the light source and the reflector. Equations (28) and (29) are equivalent to those obtained by Shealy and coworkers [28,29] for a spherical mirror by using a different procedure.

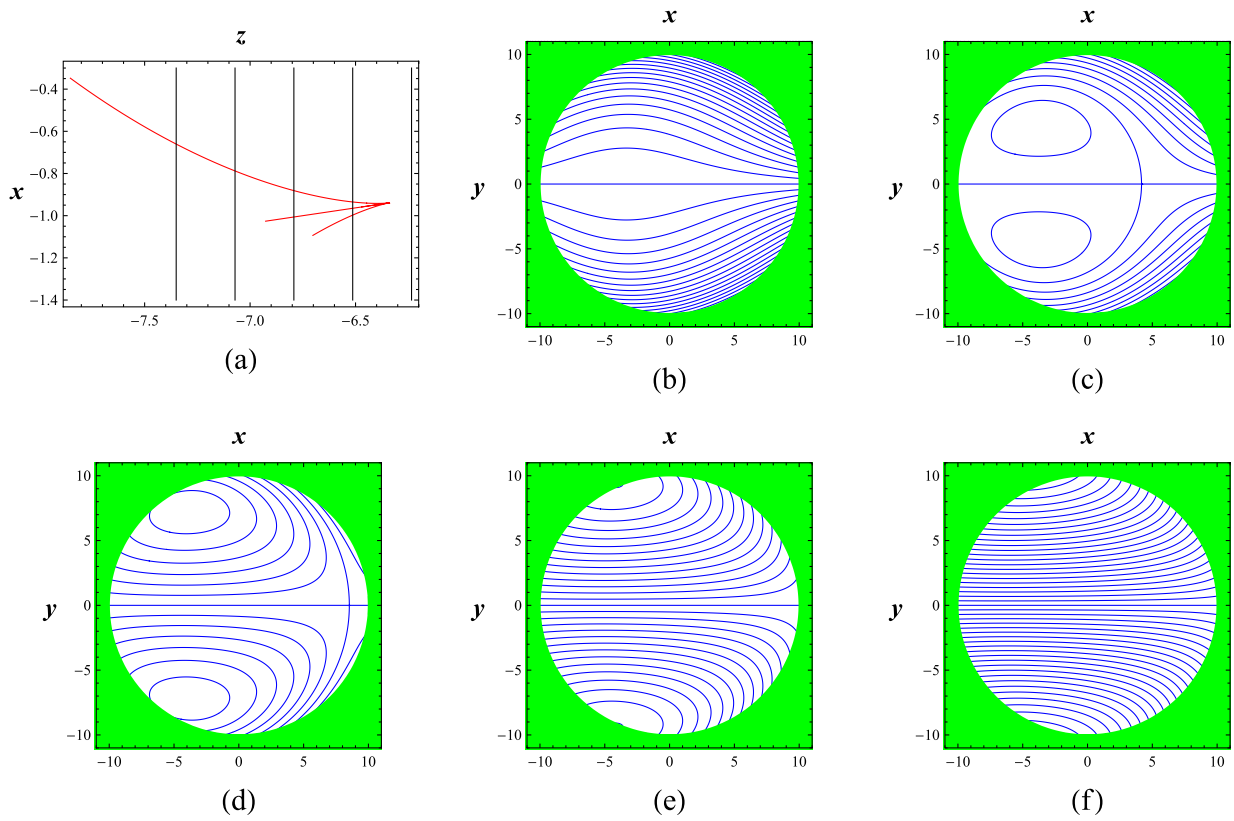

Fig. 12. (Color online) (a) Intersections of the caustic surface, given by Eqs. (28) and (29), when the point light source is placed at $\mathbf{s} = (2, 0, \text{and } 13.5 \text{ cm})$ and the planes $z =$ constant (where the Ronchi ruling is placed) with the plane $y = 0$. In (b)–(f) we present the ronchigrams when the grating is placed at the planes (b) $z = -6.23$ cm, (c) $z = -6.51$ cm, (d) $z = -6.79$ cm, (e) $z = -7.07$ cm, and (f) $z = -7.35$ cm, respectively.

C. Equations to Compute the Ideal Ronchigram

Now that we know the caustic associated with the reflected light rays by a spherical mirror when the point light source is located at an arbitrary position in the space, we finally study the structure of the ronchigram when the Ronchi ruling is placed at different relative positions to the caustic. Using Eqs. (16)–(18) we find that the equation that allows us to simulate the ideal ronchigram for a spherical mirror when the point light source is located at an arbitrary point in free space and the Ronchi ruling is placed on the plane $Z = z_0 =$ constant, with its rulings making an angle Θ with the positive T_x axis, is given by

$$y + (z_0 - f)\left(\frac{2(\mathbf{s}\cdot\mathbf{r})y - a^2(s_2 + y)}{2(\mathbf{s}\cdot\mathbf{r})f - a^2(s_3 + f)}\right) = \left[x + (z_0 - f)\left(\frac{2(\mathbf{s}\cdot\mathbf{r})x - a^2(s_1 + x)}{2(\mathbf{s}\cdot\mathbf{r})f - a^2(s_3 + f)}\right)\right]\tan\Theta + nd. \quad (30)$$

Within the geometrical optics approximation this equation is exact, and it is the equation that we use to study the structure of the ronchigrams. But before that, we present the paraxial approximation expression to this equation:

$$y(2z_0 + a) = x(2z_0 + a)\tan\Theta - nda. \quad (31)$$

Remember that in the paraxial approximation the caustic reduces to the point $(0, 0, -a/2)$. Therefore, if the Ronchi ruling is located at the caustic, that is, at the plane $Z = z_0 = -a/2$, then Eq. (31) implies that n must be zero without any restriction on the values of x, y, and Θ. In this case, the shadow coincides with the entire mirror. On the other hand, if the Ronchi ruling is not located at the caustic, that is, $(2z_0 + a) \neq 0$, then Eq. (31) can be rewritten in the following way:

$$y = x\tan\Theta - nD \quad \text{with } D \equiv \frac{da}{2z_0 + a}, \quad (32)$$

which describes a set of straight shadows making an angle Θ with the positive x axis and D is the distance between two adjacent shadows. Observe that $D = d$ when $z_0 = 0$.

D. Plots

Here we describe the caustic, the reflected wavefronts, and the ronchigrams associated with a spherical mirror when the point light source is located at different given positions to the mirror. In all the plots we assume that $a = 24.15$ cm.

1. Plots of the Caustic

To obtain the plots of the caustic for a spherical mirror, we assume that the position of the point light source is given and we use polar coordinates; that is, in Eqs. (28) and (29) we take $x = \rho\cos\varphi$ and $y = \rho\sin\varphi$, with $0 \le \rho \le 10$ cm and $0 \le \varphi \le 2\pi$.

When the point light source is placed at the center of the spherical mirror, the optical system has spherical symmetry and for this reason the reflected wavefronts associated with the reflected light rays are spherical and they will focus at the center of the mirror. As pointed out before, this point coincides with the caustic associated with the reflected light

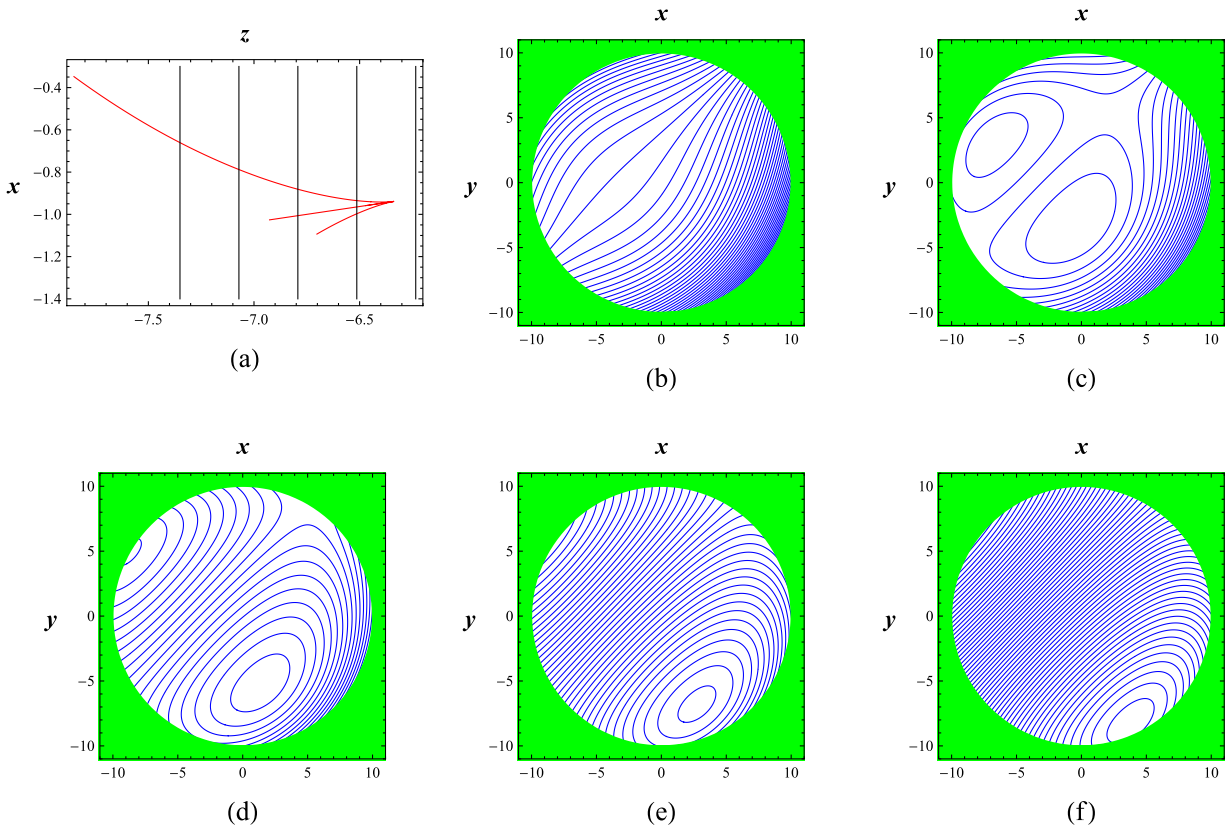

Fig. 13. (Color online) (a) Intersections of the caustic surface, given by Eqs. (28) and (29), when the point light source is placed at $\mathbf{s} = (2, 0,$ and 13.5 cm) and the planes $z =$ constant (where the Ronchi ruling is placed) with the plane $y = 0$. In (b)–(f) we present the ronchigrams when the grating is placed at the planes (b) $z = -6.23$ cm, (c) $z = -6.51$ cm, (d) $z = -6.79$ cm, (e) $z = -7.07$ cm, and (f) $z = -7.35$ cm, respectively. In this case the grating makes an angle $\pi/4$ with the T_x axis.

rays. If the point light source is shifted along the optical axis at a fixed position, the spherical symmetry is broken but there still remains a symmetry; that is, the optical system now has axial symmetry about the optical axis. For this reason the caustic is a segment of line and a two-dimensional surface of revolution with a degenerated singularity of the cusp type. These characteristics of the caustic can be seen in Figs. 3(a) and 4(a). Finally, when the point light source is moved off the optical axis to get its final fixed position, in general as can be seen from Eqs. (28) and (29) and Figs. 3(b), 3(c), 4(b), and 4(c), the caustic continues being a segment of a line and a two-dimensional surface. The fact that one branch of the caustic in general is a segment of a line is an intrinsic property associated with a spherical mirror. If the spherical mirror is deformed, for example, to a parabolical mirror, then when the point light source is off the optical axis the two branches of the caustic are two-dimensional surfaces that locally have stable singularities of well-known types [15].

2. Plots of the Reflected Wavefronts

When the point light source is placed at the center of the spherical mirror, the reflected wavefronts are spheres. If the point light source is shifted along the optical axis, the reflected wavefronts have axial symmetry about the optical axis and are such that before the caustic they are smooth, at the caustic they are singular and have self-intersections, and after the caustic they are smooth; see Fig. 5. When the point light source is placed off the optical axis, the wavefronts are singular and have self-intersections at the caustic region too; see Fig. 6.

3. Describing the Structure of the Ronchigrams

Here we describe the structure of the ronchigrams for a spherical mirror when the point light source is on and off the optical axis and the grating or Ronchi ruling is placed at different relative positions to the caustic associated with the reflected light rays. To this end, we have written a computer program in *Mathematica* to solve Eq. (30) for a spherical mirror when the point light source is on and off the optical axis; in both cases we take $a = 24.15$ cm, -10 cm $\le x \le 10$ cm, and -10 cm $\le y \le 10$ cm and the grating is placed in different planes $z = z_0 =$ constant. In order to present the results as clearly as possible, we first describe the case when the point light source is located on the optical axis and then when the point light source is off the optical axis.

When the point light source is on the optical axis the optical system has axial symmetry about the optical axis—in our case, the z axis. The caustic associated with the reflected light rays shares this symmetry (in general it is a segment of a line and a two-dimensional surface of revolution with a degenerated singularity of the cusp type). Therefore, in this case, to describe the structure of the ronchigram when the grating is placed at the caustic region, it is enough to consider the case when $\Theta = 0$—that is, we need to compute the level curves of T_y. Observe that the intersections of the caustic with planes $z =$ constant are of two different types. The first type is

a circle and an isolated point that coincides with the center of that circle, and the second type is a circle.

Now we describe the structure of the ronchigram associated with the first type of intersection. To this end, we take $\mathbf{s} = (0, 0, \text{and } 13.5 \text{ cm})$ and in the object space $(T_x, T_y, -6.51 \text{ cm})$ we plot the object, in our case the ruling and the caustic; the caustic is a circle of radius equal to $R_a = 0.0213$ cm and an isolated point that coincides with the center of the circle. After that, Eq. (30) is solved for x and y. Finally, the values obtained for x and y are plotted in the plane $z = 0$. In Fig. 7(a) we show the caustic and the Ronchi rulings, while in Fig. 7(b) we show the shadows of the rulings;that is, the ronchigram. As can be seen in Fig. 7(b), the ronchigram has closed-loop shadows. We remark that in accordance with the caustic touching theorem they can be interpreted as image disruptions. To show up this property we compute the shadow corresponding to some ruling bands. In Fig. 8(a), we show the caustic and the ruling corresponding to the case $nd = -(1.2)R_a$. Since the ruling is outside the caustic, there is a one-to-one correspondence between the points of the ruling and the points of its shadow, which is plotted in Fig. 8(e). The ruling is tangent to the caustic, the circle, in the object space at the point $(0 \text{ cm}, -R_a, -6.51 \text{ cm})$ [Figs. 8(b) and 8(c)]; at this point there is an image disruption of the elliptic type, which is a loop born from an isolated point; see Figs. 8(f) and 8(g). There is another image disruption at the origin of coordinates; this is so because this point belongs to the caustic too. In this case, the shadow of the ruling is a circle and a segment of line parallel to the x axis; see Figs. 8(d) and 8(h). Here it is important to remark that the circle observed in Fig. 8(h) is the shadow or image of the single point of the ruling (0, 0, and −6.51 cm). Finally, at the point $(0 \text{ cm}, R_a, -6.51 \text{ cm})$ the last image disruption appears, this time of hyperbolic type—that is, a loop pinched off from an already existing one.

Now we describe the structure of the ronchigram associated with the second type of intersection. To this end, we take $\mathbf{s} = (0, 0, \text{and } 13.5 \text{ cm})$ and in the object space $(T_x, T_y, -6.79 \text{ cm})$ we plot the rulings and the caustic that is a circle of radius equal to $R_b = 0.1142$ cm. In Fig. 9(a) we show the caustic and the Ronchi rulings, while in Fig. 9(b) we show the associated ronchigram. To understand how it is formed, as in the previous case we compute the shadow of some particular rulings. In Fig. 10(a) we show the caustic and the ruling for the case $nd = -(1.2)R_b$; in this case there are no reflected light rays connecting the ruling, and then as can be seen in Fig. 10(e) there is no shadow or image associated with this ruling. The ruling is tangent to the caustic, the circle, in the object space at the point $(0 \text{ cm}, -R_b, -6.79 \text{ cm})$ [see Fig. 10(b)]; at this point there is an image disruption of the elliptic type—that is, a loop born from an isolated point—and because of the dimensions of the mirror in this case we can observe only the isolated point corresponding to the born image; see Fig. 8(f). In Fig. 10(c) we have the ruling corresponding to the case $nd = -(1/2)R_b$ and in Fig. 8(g) we have presented its corresponding image as we can see the image that was born has evolved to a loop. In Fig. 10(d) we present the ruling corresponding to the case $nd = 0$, and in Fig. 10(h) we have that its image is a single segment of a line. Finally, in Fig. 11 we present the ronchigrams when the point light source is at $\mathbf{s} = (0, 0, \text{and } 13.5 \text{ cm})$ and the grating is placed at different positions on the optical axis.

When the point light source is placed out off the optical axis, the axial symmetry of the optical system is broken. Therefore, to study the structure of the ronchigram when the Ronchi ruling is placed at the caustic region, we assume that $\mathbf{s} = (2, 0, 13.5 \text{ cm})$ and we consider two different subcases; in the first we take $\Theta = 0$, and in the second $\Theta = \pi/4$. The results for $\Theta = 0$ are shown in Fig. 12, and for $\Theta = \pi/4$ they are shown in Fig. 13. In order to appreciate the differences between the ronchigrams when the point light source is on and off the optical axis, we have placed the Ronchi ruling in exactly the same $z =$ constant plane to obtain Figs. 11–13. From Fig. 12 we can see that the effect of taking the point light source off the optical axis on the ronchigrams is a kind of translation along the positive x axis. Finally, from Fig. 13 we see that the rotation of the Ronchi ruling produces a ronchigram that is also rotated.

It is important to point out that to generate Figs. 11–13 we have assumed that the grating is such that $-3 \text{ cm} \le T_x \le 3 \text{ cm}$, and $d = 0.02$ cm.

4. CONCLUSIONS

In this work we have used our general results on the wavefronts and the caustic associated with the light rays reflected by an arbitrary smooth mirror after being emitted by a point light source located at an arbitrary position in free space to obtain compact *analytical* expressions for the reflected wavefronts and caustic surface for a spherical mirror. We found that in general the caustic is a segment of line and a two-dimensional surface. This result implies that the caustic for the spherical mirror is not stable under a small deformation of the spherical surface. Furthermore, we obtained the equations that allow us to compute the ronchigram when the point light source is placed at an arbitrary position in space. We obtained the ronchigram when the grating is placed at different relative position to the caustic region. When the grating is placed at the caustic region, the ronchigram contains closed-loop fringes. These fringes appear when the grating becomes tangent to the caustic region. Finally, from Figs. 11–13 we conclude that in general if the caustic is a closed curve, for example, a circle, then the image or shadow of each Ronchi ruling that crosses the caustic in general is two curves: one is open, and the other one is a loop.

ACKNOWLEDGMENTS

Ramón Silva-Ortigoza, Mariana Marcelino-Aranda, and Magdalena Marciano-Melchor acknowledge financial support from SNI (Sistema Nacional de Investigadores), Secretaría de Investigación y Posgrado (SIP) of Instituto Politécnico Nacional (IPN), and the programs EDI, EDD, and COFAA of IPN. José Guadalupe Santiago-Santiago, Román Suárez-Xique, and José Miguel Zárate-Paz were supported by a CONACyT scholarship. Gilberto Silva-Ortigoza acknowledges financial support from SNI. This work has received partial support from VIEP-BUAP. Edwin Román-Hernández acknowledges financial support from PROMEP (UNISTMO-PTC-071, 103.5/12/3718).

REFERENCES

1. D. Malacara, A. Cornejo, and M. V. R. K. Murty, "Bibliography of various optical testing methods," Appl. Opt. **14**, 1065–1065 (1975).

2. A. Cornejo, H. J. Caulfied, and W. Friday, "Testing of optical surfaces: a bibliography," Appl. Opt. **20**, 4148–4148 (1981).
3. V. Ronchi, "Forty years of history of a grating interferometer," Appl. Opt. **3**, 437–451 (1964).
4. A. Cornejo-Rodriguez, "Ronchi test," in *Optical Shop Testing*, D. Malacara, ed. (Wiley, 1978), Chap. 9.
5. A. A. Sherwood, "Quantitative analysis of the Ronchi test in terms of Ray optics," J. Br. Astron. Assc. **68**, 180–191 (1958).
6. A. A. Sherwood, "Ronchi test charts for parabolic mirrors," J. Proc. R. Soc. N. S. W. **93**, 19–23 (1959).
7. D. Malacara and A. Cornejo, "Null Ronchi test for aspherical surfaces," Appl. Opt. **13**, 1778–1780 (1974).
8. T. Yatagai, "Fringe scanning Ronchi test for aspherical surfaces," Appl. Opt. **23**, 3676–3679 (1984).
9. A. Cordero-Dávila, A. Cornejo-Rodriguez, and O. Cardona-Nuñez, "Null Hartmann and Ronchi–Hartmann tests," Appl. Opt. **29**, 4618–4621 (1990).
10. A. Cordero-Dávila, A. Cornejo-Rodriguez, and O. Cardona-Nuñez, "Ronchi and Hartmann tests with the same mathematical theory," Appl. Opt. **31**, 2370–2376 (1992).
11. A. Cordero-Dávila, J. Daz-Anzures, and V. Cabrera-Peláez, "Algorithm for the simulation of ronchigrams of arbitrary optical systems and Ronchi grids in generalized coordinates," Appl. Opt. **41**, 3866–3873 (2002).
12. E. Román-Hernández and G. Silva-Ortigoza, "Exact computation of image disruption under reflection on a smooth surface and Ronchigrams," Appl. Opt. **47**, 5500–5518 (2008).
13. M. V. Berry, "Disruption of images: the caustic-touching theorem," J. Opt. Soc. Am. A **4**, 561–569 (1987).
14. E. Román-Hernández, J. G. Santiago-Santiago, G. Silva-Ortigoza, and R. Silva-Ortigoza, "Wavefronts and caustic of a spherical wave reflected by an arbitrary smooth surface," J. Opt. Soc. Am. A **26**, 2295–2305 (2009).
15. E. Román-Hernández, J. G. Santiago-Santiago, G. Silva-Ortigoza, R. Silva-Ortigoza, and J. Velázquez-Castro, "Describing the structure of ronchigrams when the grating is placed at the caustic region: the parabolical mirror," J. Opt. Soc. Am. A **27**, 832–845 (2010).
16. M. Mansuripur, "The Ronchi test," Opt. Photon. News **8**, 42–46 (1997).
17. D. Malacara, "Geometrical Ronchi test of aspherical mirrors," Appl. Opt. **4**, 1371–1374 (1965).
18. V. I. Arnold, *Catastrophe Theory* (Springer-Verlag, 1986).
19. V. I. Arnold, S. M. Gusein-Zade, and A. N. Varchenko, *Singularities of Differentiable Maps* (Birkhauser, 1995).
20. V. I. Arnold, *Mathematical Methods of Classical Mechanics* (Springer-Verlag, 1980).
21. D. L. Shealy and D. G. Burkhard, "Caustic surfaces and irradiance for reflection and refraction from an ellipsoid, elliptic paraboloid, and elliptic cone," Appl. Opt. **12**, 2955–2959 (1973).
22. D. G. Burkhard and D. L. Shealy, "Simplified formula for the illuminance in an optical system," Appl. Opt. **20**, 897–909 (1981).
23. P. S. Theocaris, "Surface topography by caustics," Appl. Opt. **15**, 1629–1638 (1976).
24. P. S. Theocaris, Properties of caustics from conic reflectors. 1: meridional rays," Appl. Opt. **16**, 1705–1716 (1977).
25. G. Silva-Ortigoza, J. Castro-Ramos, and A. Cordero-Dávila, "Exact calculation of the circle of least confusion of a rotationally symmetric mirror. II," Appl. Opt. **40**, 1021–1028 (2001).
26. G. Silva-Ortigoza, M. Marciano-Melchor, O. Carvente-Muñoz, and Ramón Silva-Ortigoza, "Exact computation of the caustic associated with the evolution of an aberrated wavefront," J. Opt. A **4**, 358–365 (2002).
27. J. Castro-Ramos, O. de Ita Prieto, and G. Silva-Ortigoza, "Computation of the disk of least confusion for conic mirrors," Appl. Opt. **43**, 6080–6088 (2004).
28. D. L. Shealy and D. G. Burkhard, "Flux density ray propagation in discrete index media expressed in terms of the intrinsic geometry of the reflecting surface," Opt. Acta **20**, 287–301 (1973).
29. D. L. Shealy, "Analytical illuminance and caustic surface calculations in geometrical optics," Appl. Opt. **15**, 2588–2596 (1976).